

~~CONFIDENTIAL~~

NACA RM L51I28



RESEARCH MEMORANDUM

ROCKET-MODEL INVESTIGATION OF THE ROLLING EFFECTIVENESS
OF A FIGHTER-TYPE WING-CONTROL CONFIGURATION

AT MACH NUMBERS FROM 0.6 TO 1.5

By H. Kurt Strass and Edward T. Marley

Langley Aeronautical Laboratory
Langley Field, Va.

*NASA Lab. dated 6-16-83 JTB/RSS
SKM 498*

CLASSIFIED DOCUMENT

This material contains information affecting the National Defense of the United States within the meaning of the espionage laws, Title 18, U.S.C., Secs. 793 and 794, the transmission or revelation of which in any manner to unauthorized person is prohibited by law.

NATIONAL ADVISORY COMMITTEE FOR AERONAUTICS

WASHINGTON

February 25, 1952

~~CONFIDENTIAL~~



NATIONAL ADVISORY COMMITTEE FOR AERONAUTICS

RESEARCH MEMORANDUM

ROCKET-MODEL INVESTIGATION OF THE ROLLING EFFECTIVENESS
OF A FIGHTER-TYPE WING-CONTROL CONFIGURATION
AT MACH NUMBERS FROM 0.6 TO 1.5

By H. Kurt Strass and Edward T. Marley

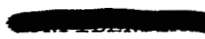
SUMMARY

An investigation of the rolling effectiveness of spoiler and aileron aerodynamic controls on a fighter-type airplane has been conducted at Mach numbers from 0.6 to 1.5 by the Langley Pilotless Aircraft Research Division by utilizing rocket-propelled test vehicles.

No effects of mutual interference between the midspan spoiler and the outboard aileron were detectable. Above the speed of sound, the ailerons were relatively ineffective as compared with the spoiler because of wing twisting. For conditions of equal rolling effectiveness, the twisting-moment coefficient of the aileron was approximately three times that of the spoiler.

INTRODUCTION

An investigation has been made, by means of rocket-powered models in free flight, of the rolling effectiveness of a wing-control configuration planned for a fighter-type airplane. Rolling effectiveness and drag measurements were obtained at Mach numbers from 0.6 to 1.5 with the controls mounted upon wings which approximated the scaled structural characteristics estimated for the airplane. The rolling-effectiveness results are compared with experimentally determined rigid-wing values.



b	diameter of circle swept by wing tips, 2.85 feet
c_m	section pitching-moment coefficient
c	wing chord parallel to model center line, inches
D	drag of test model, pounds
h	spoiler projection above wing surface normal to chord plane, inches
M	Mach number
m	concentrated couple applied near wing tip in a plane perpendicular to both the 41.7-percent-chord line (main spar location) and the wing chord plane, inch-pounds
P	static pressure, pounds per square foot
P_l	concentrated load applied on the 41.7-percent-chord line at $\frac{y}{b/2} = 0.925$, pounds
p	rolling velocity, radians per second
q	dynamic pressure, pounds per square foot
S_2	area of two wing panels measured to fuselage center line, 2.70 square feet
S_3	exposed area of three wing panels, 3.29 square feet
V	flight-path velocity, feet per second
y	distance to 41.7-percent-chord line, measured perpendicular to model center line, feet
α	angle of attack
δ_p	deflection of test wing along 41.7-percent-chord line under load P_l , inches
δ_a	deflection of each aileron in a plane perpendicular to the aileron hinge line

i_w	average wing incidence for three wings measured in plane parallel to the direction of flight, positive when tending to produce clockwise roll as seen from the rear, degrees
θ	angle of twist due to m , radians
h/c	spoiler extension above wing surface in local chord lengths
$\delta p/P_L$	wing bending-stiffness parameter, inches per pound
θ/m	wing torsional-stiffness parameter, radians per inch-pound
$p_b/2V$	wing tip helix angle, radians
$c_{m\delta}/\alpha_\delta$	effective section twisting-moment coefficient per unit rolling effectiveness
C_{DT}	total drag coefficient $\left(\frac{D}{qS_3}\right)$

Subscripts:

a	at altitude of test
av	average
o	at sea level
r	at reference station (mid-control)
δ	per degree of aileron deflection

MODELS AND TECHNIQUE

The geometric characteristics of the test vehicles used in this investigation are described in the sketches and photographs of figures 1 to 5.

The airfoil sections used on the configurations tested were the NACA 0009-1.16 38/1.14 (modified) at the root and the NACA 0007-1.16 38/1.14 (modified) at the tip. The aspect ratio b^2/S_2 for all models tested was 3.02. Both wings of the proposed airplane are equipped with upper-surface spoilers and boundary-layer control fences, lower-surface tip skids, and plain partial-span trailing-edge ailerons. During most rolling maneuvers, an unsymmetric condition occurs which could not be duplicated with a single three-wing test vehicle of the present type, so several models were flown to test the airplane right and left wing

panels independently. The various control configurations are illustrated schematically in figure 5. The type A model simulates the right wing of the airplane when the spoiler and aileron are set to cause the airplane to roll to the right. Type B is similar, but only the spoiler is extended. Type C simulates the left wing of the airplane when the airplane is in right roll. For simplicity, the test model was constructed in a manner to cause the model with a right wing to roll to the left, as is illustrated. This is of no importance because the relative location of the boundary-control fence and the wing tip skid is the same as that for the airplane left wing panel in right roll.

An important phase of this investigation was the determination of the effects of aeroelasticity upon the rolling effectiveness. To do this, a stiff model and a flexible model were constructed for every wing-control configuration. The stiff models were as stiff as could feasibly be made in order to minimize aeroelastic effects, whereas the flexible models were constructed in a manner to approximate the scaled structural characteristics estimated for the proposed airplane. The data from the stiff and flexible models were cross plotted against wing torsional stiffness and the values for the rolling effectiveness at infinite rigidity were obtained by extrapolation. The structural details of the two types of wing construction are shown in figure 4. The surface finish of all models was highly polished lacquer with a minimum of waviness.

The technique used to measure the model structural characteristics is illustrated in figure 6, which presents a typical test set-up of the type used for determination of the spanwise variation of the torsional stiffness parameter θ/m . The variation of the flexural stiffness parameter δ_p/P_L with span was determined in a similar manner with the substitution of a concentrated load on the 41.7-percent-chord line (location of main spar) near the wing tip for the torque transfer yoke illustrated in the photograph.

The flight tests were made at the Langley Pilotless Aircraft Research Station at Wallops Island, Va. The test vehicles were propelled by a two-stage rocket propulsion system to a Mach number of about 1.5. All data were obtained during a period of approximately 10 seconds of coasting flight following rocket-motor burnout. Time histories of the rolling velocity were obtained with special radio equipment. The flight-path velocity was obtained with CW Doppler radar and the space coordinates with SCR 584 radar. These data, in conjunction with atmospheric data obtained by means of radiosonde, permit the evaluation of the aileron rolling effectiveness $pb/2V$ and the total drag coefficient C_{DT} as a function of Mach number. The Reynolds number for the tests varied from approximately 3×10^6 at $M = 0.6$ to 9×10^6 at $M = 1.5$. For a more complete description of the flight testing technique, see reference 1.

ACCURACY AND CORRECTIONS

Based upon previous experience, the maximum experimental error is estimated to be within the following limits:

	<u>Subsonic</u>	<u>Supersonic</u>
C_{DT}	±0.004	±0.002
$pb/2V$, radians	±0.004	±0.002
M	±0.005	±0.005

The sensitivity of the experimental technique, however, is such that much smaller irregularities in the variation of $pb/2V$ with Mach number may be detected. For purposes of economy and ease of construction, small variations from the desired values of 0° and 5° for wing incidence and control deflection, respectively, were permitted. The data were adjusted for effect of wing incidence by use of the equation given in reference 2, which was derived from strip theory for rigid wings. The adjustments for aileron deflection were made by reducing the data to $\frac{pb/2V}{\delta_a}$ and then multiplying by the nominal δ_a value of 5° . For the case of the aileron and spoiler in combination, adjustment was made only for that portion contributed by the aileron. The actual measured values for the models tested are presented in table I in order to show the magnitude of such adjustments.

No attempt was made to correct for the effect of the test-vehicle moment of inertia about the roll axis on the measured variation of $pb/2V$ with Mach number, since the analysis in reference 1 indicated that the magnitude of the correction is small enough not to affect the conclusions drawn from these data.

RESULTS AND DISCUSSION

Basic data.- The structural and aerodynamic data obtained during this investigation are presented in figure 7. The measured distributions of the stiffness of the wings in bending and torsion are presented as plots of δ_p/P_l , the bending-stiffness parameter, and θ/m , the torsional-stiffness parameter, against $\frac{y}{b/2}$. The structural characteristics

estimated for a typical airplane have been scaled down to allow comparison with the measured characteristics of the test models. The variation of θ/m (measured parallel to the direction of flight) with $\frac{y}{b/2}$ has been included to allow use of the method presented in reference 3 to obtain effective twisting-moment coefficients. The static pressure existing during each flight is also shown on the figure as the variation of P_a/P_0 with Mach number, where P_a/P_0 is the ratio of static pressure at the altitude of the test to standard sea-level pressure (2116 pounds per square foot). The aerodynamic results obtained are presented as the variation of $pb/2V$, the control rolling effectiveness, and C_{DT} , the total drag coefficient, with Mach number.

Because different atmospheric conditions prevailed for the various tests, and because the data were obtained over an altitude range of approximately 10,000 feet, it was necessary to correct all of the rolling-effectiveness data to standard sea-level conditions to provide an adequate basis for comparison. This correction was made in a manner similar to the method described in reference 3.

Rolling effectiveness.- The effect of wing flexibility upon rolling effectiveness corrected to sea-level conditions is presented in figure 8. The rigid-wing values were obtained by extrapolation from cross plots of $pb/2V$ against wing torsional stiffness. These data are summarized in figure 9 to allow direct comparison between the various wing-control configurations. It is noted that above the speed of sound the aileron was relatively ineffective as compared with the spoiler because of wing twisting. In addition, a comparison is made of the measured rolling effectiveness for the combined aileron and spoiler A with that obtained from the summation of the results of the aileron and spoiler A tested separately. The excellent agreement between these values indicates that the mutual interference between the midspan spoiler and the outboard aileron was very small.

Figure 10 presents the variation of the effective section twisting-moment coefficient $c_{m\delta}/\alpha_\delta$ (see reference 3) with Mach number for the spoiler-alone and aileron-alone configurations. Since α_δ is proportional to the rolling effectiveness, the comparatively low values of $c_{m\delta}/\alpha_\delta$ obtained for the spoiler (about one-third as large as those for the aileron) illustrate a possible merit of spoilers for control where wing twisting is a problem.

Drag.- A comparison of the results from the stiff-wing configurations with those from the flexible-wing configurations, to show the effect of wing flexibility upon the variation of the total drag coefficient C_{DT}

with Mach number, is presented in figure 11. In every case the flexible models had less drag than the comparable stiff models. It is interesting to note that the increment in drag coefficient due to the increase in wing stiffness for the configuration which employed the aileron and spoiler in combination is approximately equal to the sum of the increments for the controls tested separately. This is illustrated in figure 11(a), in which the estimated variation of C_{DT} with M obtained by subtracting the sum of the incremental values from the stiff-wing results is compared with the measured flexible-wing data.

The effect of the type of control upon the variation of C_{DT} with M is presented in figure 12 for the stiff- and flexible-wing models. The most significant fact about these data is the extremely large increase in C_{DT} which accompanied the use of the spoiler. At speeds less than $M \approx 0.95$, the drag of the spoiler configuration was more than twice that of the aileron configuration; for speeds greater than $M \approx 0.95$, the drag was approximately 20 percent greater.

Effect of gap upon spoiler performance.- Figure 13 presents a comparison of two types of spoilers that were tested in combination with ailerons on the stiff wings. The spoiler A was similar to that planned for use upon the proposed airplane, whereas for spoiler B, the spanwise variation of the extension of the spoiler above the wing surface differed slightly from spoiler A and there was no gap between the lower surface of the spoiler and the wing surface as employed by spoiler A. As the average extension of the two types of spoilers was very nearly the same (for spoiler A, $(h/c)_{av} = 0.063$; for spoiler B, $(h/c)_{av} = 0.0614$), the differences in the values of $pb/2V$ and C_{DT} which were obtained for the two controls are attributable primarily to the effect of the gap. The gap caused an appreciable increase in $pb/2V$ at Mach numbers below $M \approx 1.36$ and indications of a decrease above $M \approx 1.36$. The effect of the gap upon the total drag coefficient was a decrease of approximately 25 percent in the subsonic region and approximately 10 percent in the supersonic region.

CONCLUSIONS

An investigation, by means of rocket-powered models, of the rolling effectiveness of a wing-control configuration simulating a fighter-type airplane indicates the following conclusions:

1. Within the experimental accuracy, no mutual interference with respect to rolling effectiveness was detectable between the midspan spoiler and the outboard aileron.

2. Above the speed of sound, the ailerons were relatively ineffective as compared with the spoiler because of wing twisting.

3. The results indicate that, for equal rolling effectiveness, the aileron had approximately three times the effective wing twisting-moment coefficient of the spoiler.

4. For equal rolling effectiveness the use of the spoiler was accompanied by an extremely large increase in the total drag coefficient as compared with that for the aileron.

Langley Aeronautical Laboratory
National Advisory Committee for Aeronautics
Langley Field, Va.

REFERENCES

1. Sandahl, Carl A., and Marino, Alfred A.: Free-Flight Investigation of Control Effectiveness of Full-Span 0.2-Chord Plain Ailerons at High Subsonic, Transonic, and Supersonic Speeds to Determine Some Effects of Section Thickness and Wing Sweepback. NACA RM L7D02, 1947.
2. Strass, H. Kurt, and Marley, Edward T.: Rolling Effectiveness of All-Movable Wings at Small Angles of Incidence at Mach Numbers from 0.6 to 1.6. NACA RM L51H03, 1951.
3. Strass, H. Kurt, Fields, E. M., and Purser, Paul E.: Experimental Determination of Effect of Structural Rigidity on Rolling Effectiveness of Some Straight and Swept Wings at Mach Numbers from 0.7 to 1.7. NACA RM L50G14b, 1950.

TABLE I

Wing-control configuration	Type	Construction	Model	i_w (deg)	δ_a (deg)	Figure
Spoiler A	B	Flexible	1	-0.01	-----	7(a)
Aileron	C	Flexible	1	-.04	-5.14	7(b)
Aileron + spoiler A	A	Flexible	1	.07	4.96	7(c)
Spoiler A	B	Stiff	1	-.01	-----	7(d)
Aileron	C	Stiff	1	.07	-5.15	7(e)
Aileron	C	Stiff	2	-.01	-5.15	7(e)
Aileron + spoiler A	A	Stiff	1	0	4.85	7(f) 7(g)
Aileron + spoiler A	A	Stiff	2	.10	4.76	7(f) 7(g)
Aileron + spoiler B	A	Stiff	1	.15	4.90	7(g)



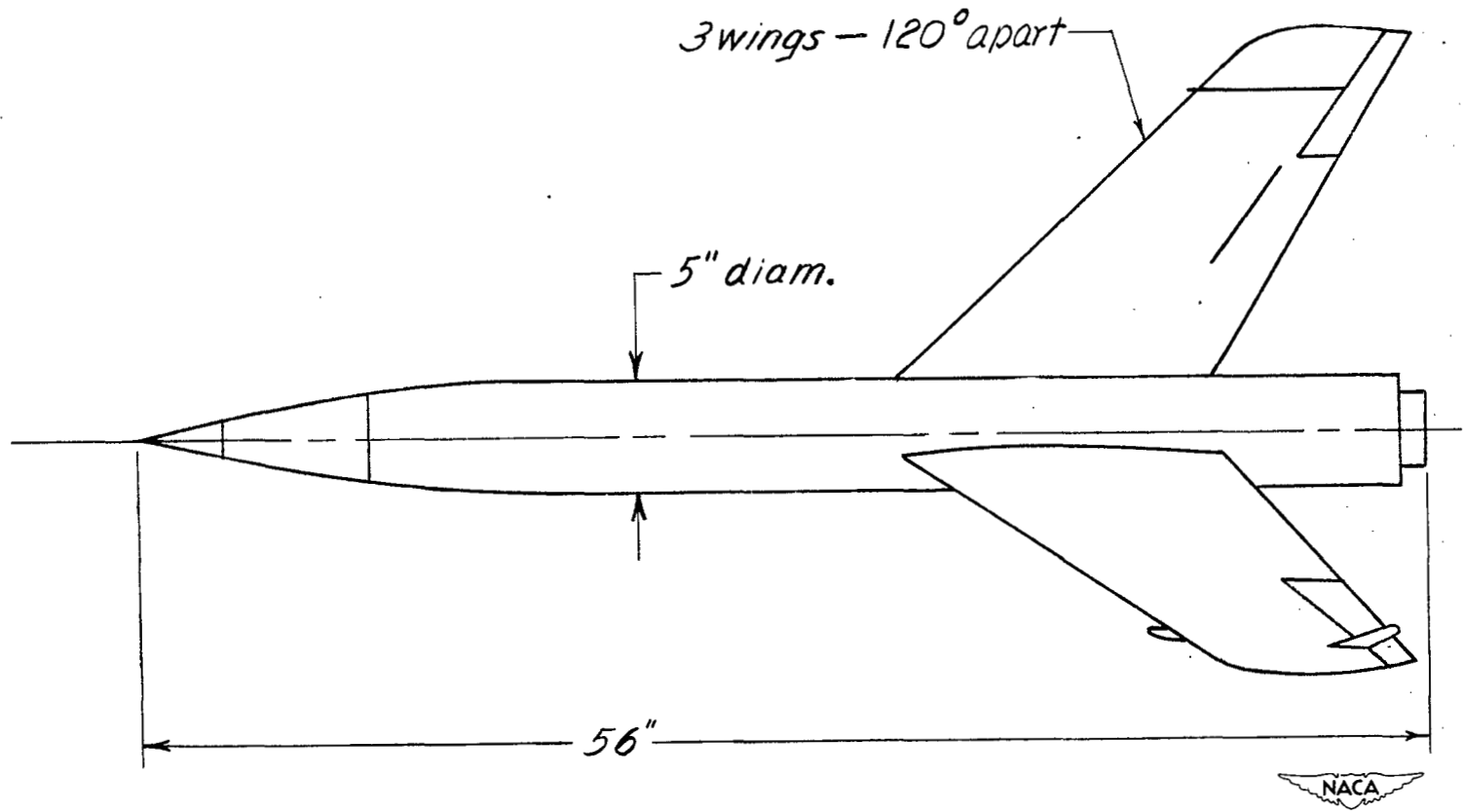


Figure 1.- General arrangement of test vehicle.

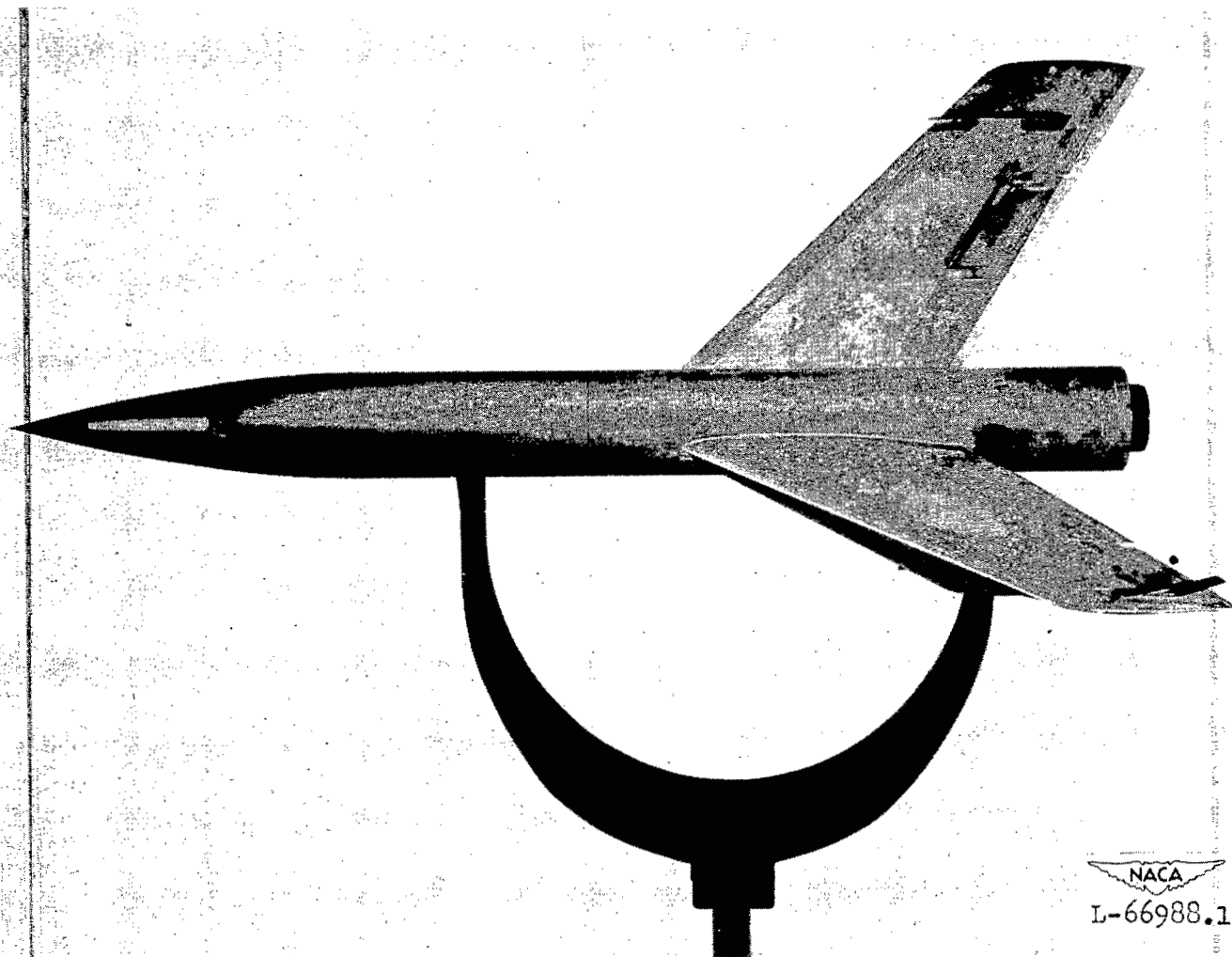
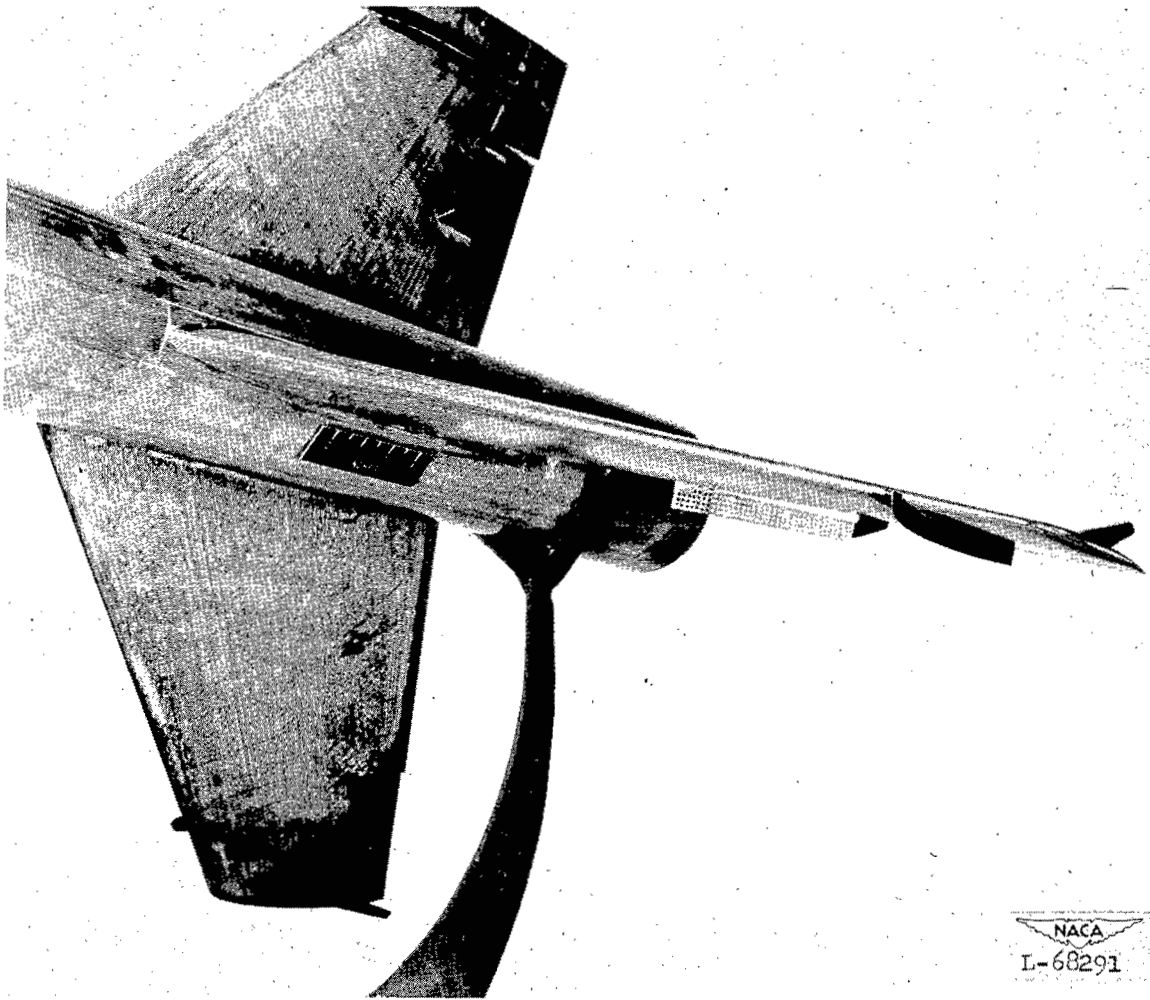
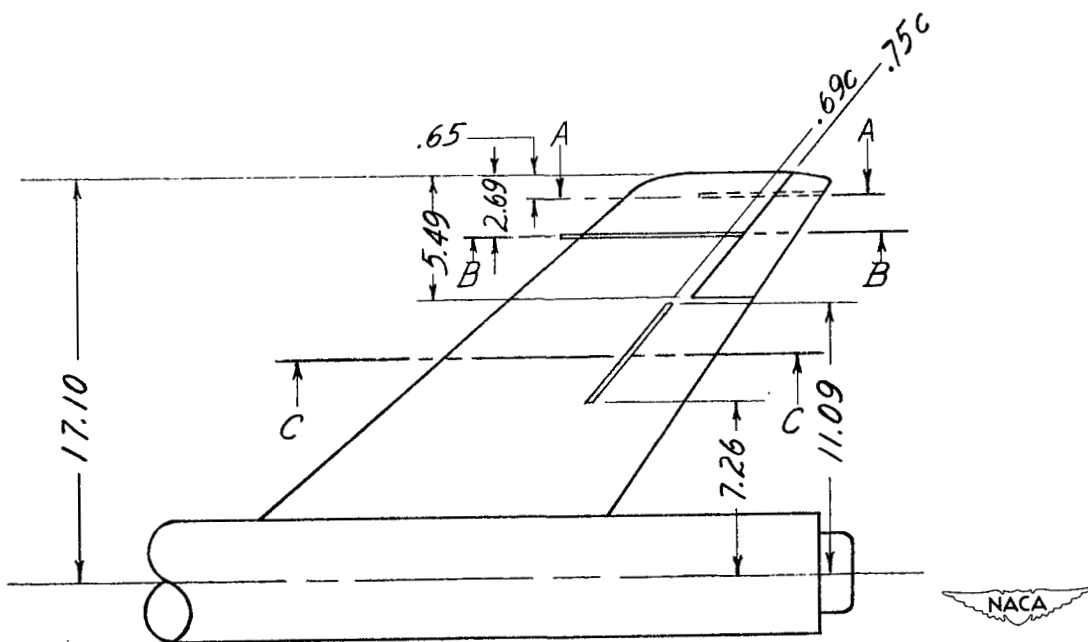
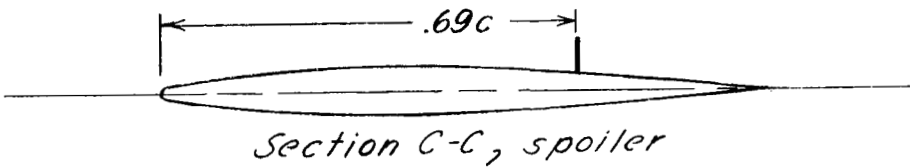
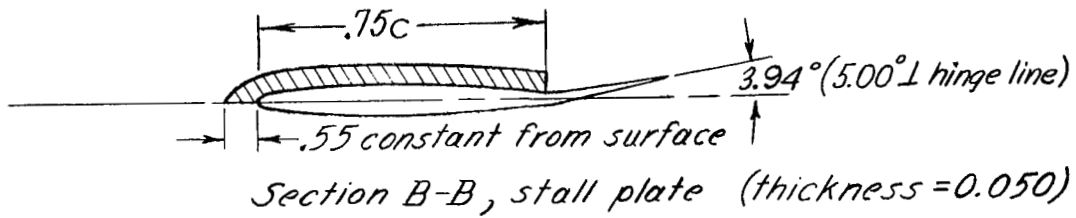
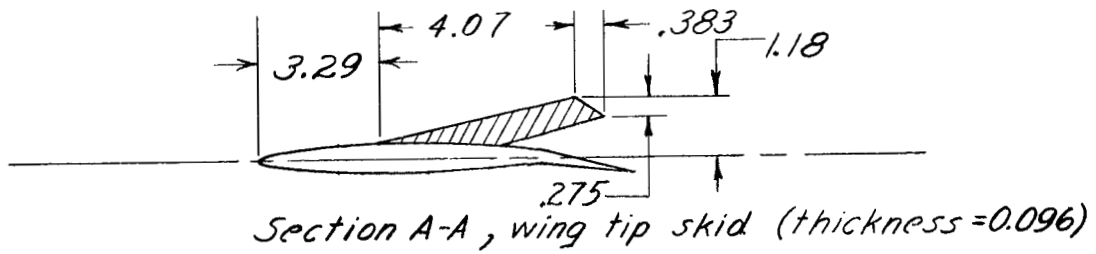


Figure 2.- Typical test vehicle.



NACA
L-68291

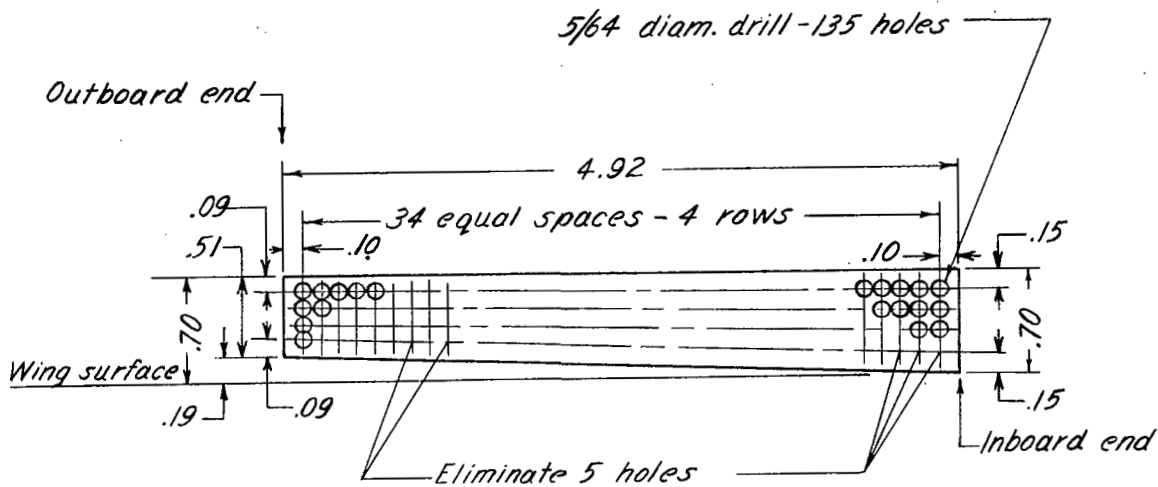
Figure 3.- Close-up of wings and controls.



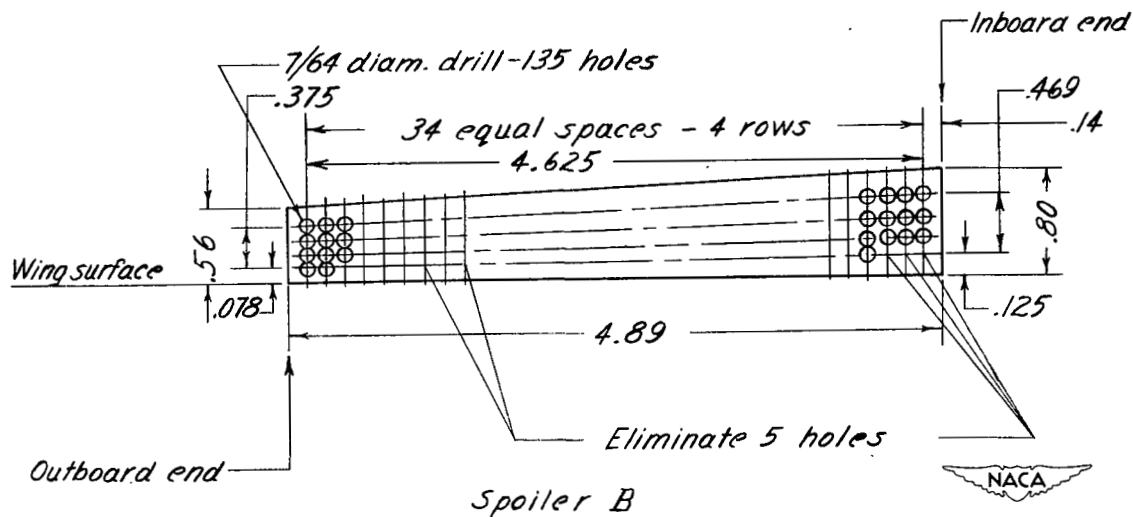
(a) External details.

Figure 4.- Description of wings and controls. All dimensions are in inches.



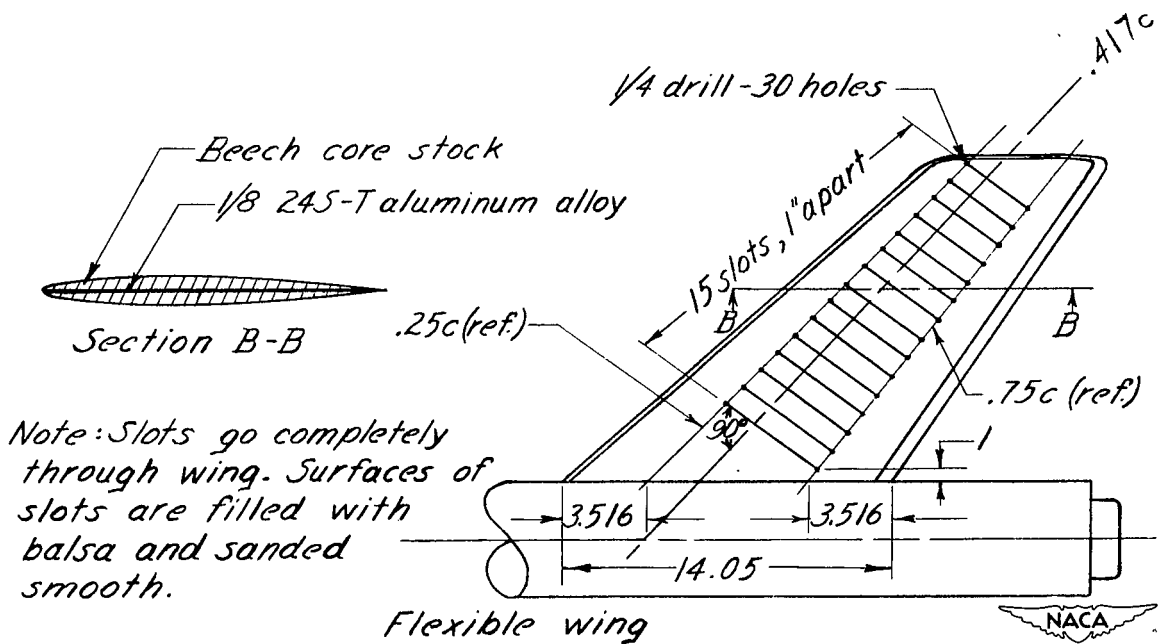
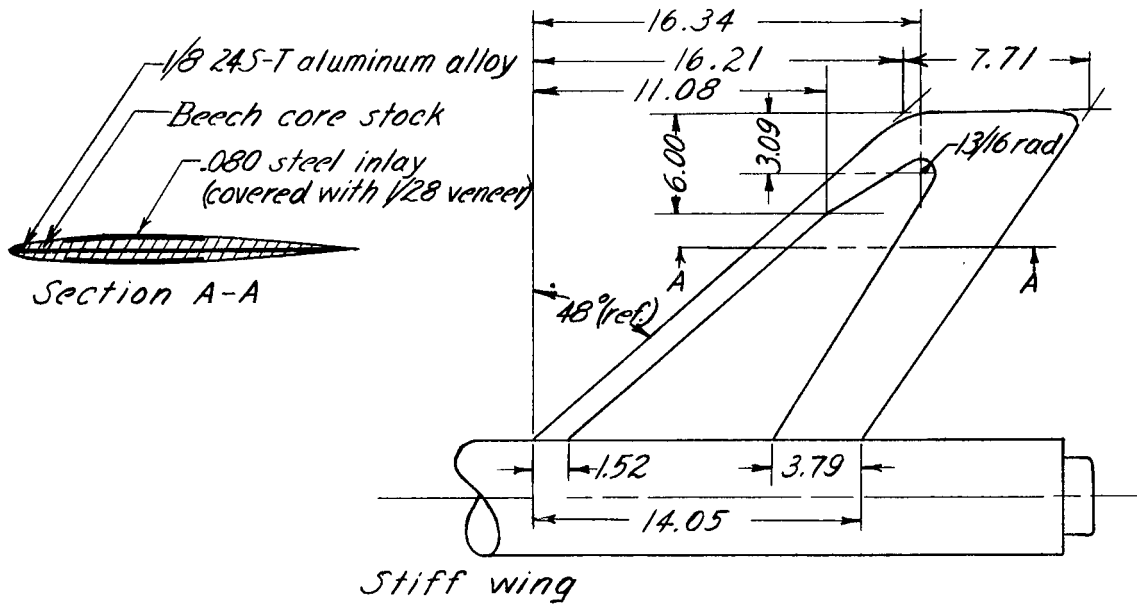


Spoiler A



(b) Spoiler details (thickness = 0.062).

Figure 4.- Continued.



(c) Structural details.

Figure 4.- Concluded.

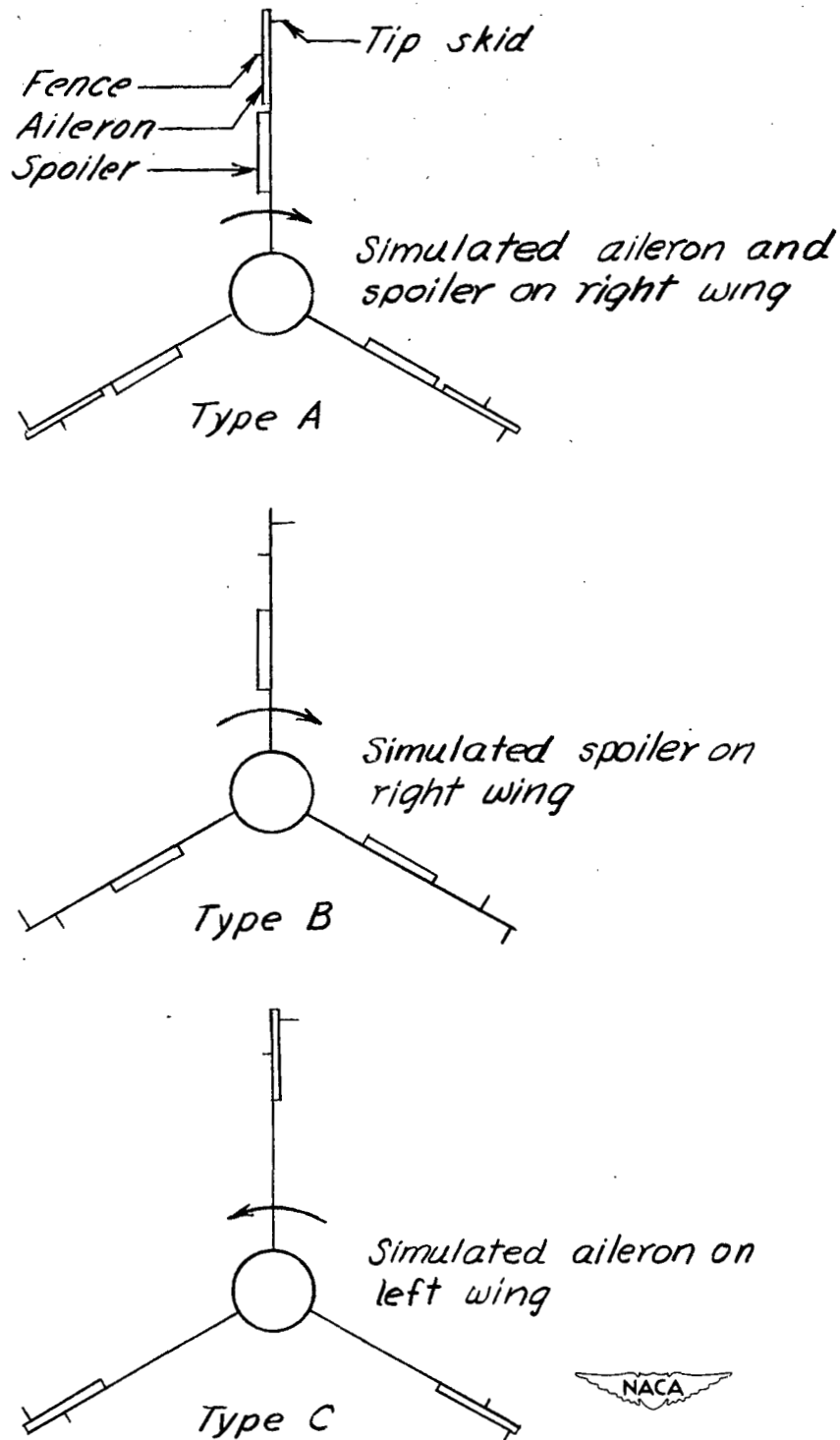


Figure 5.- Schematic illustration of the control combinations tested as seen from rear of test vehicle. Arrows show direction of positive rotation.

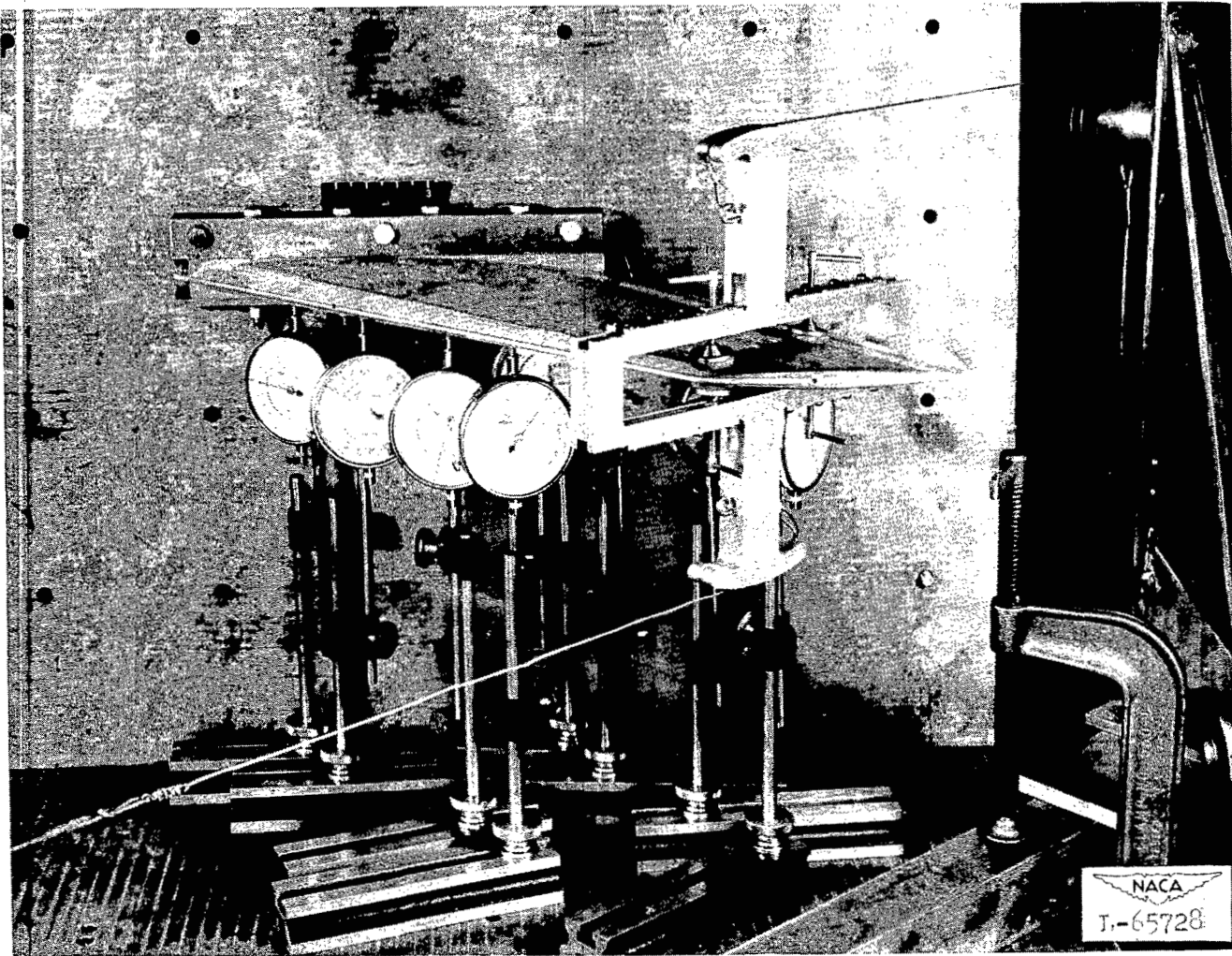
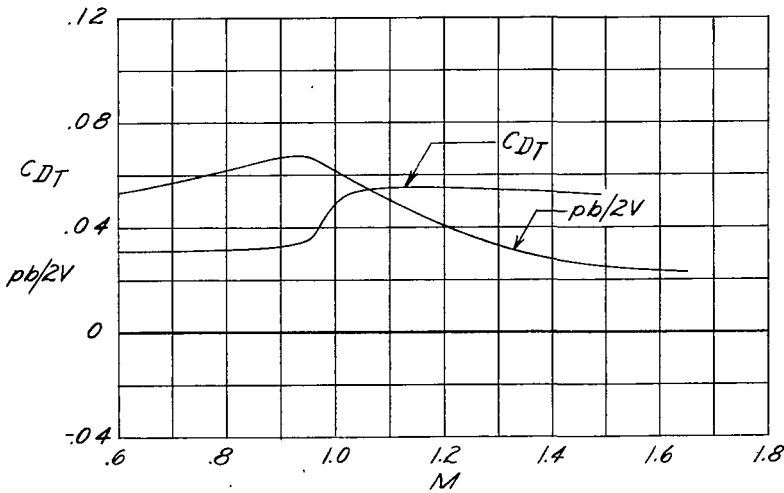
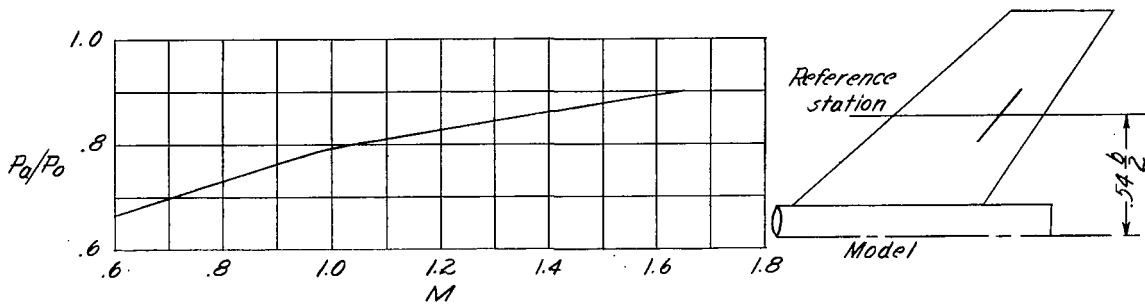
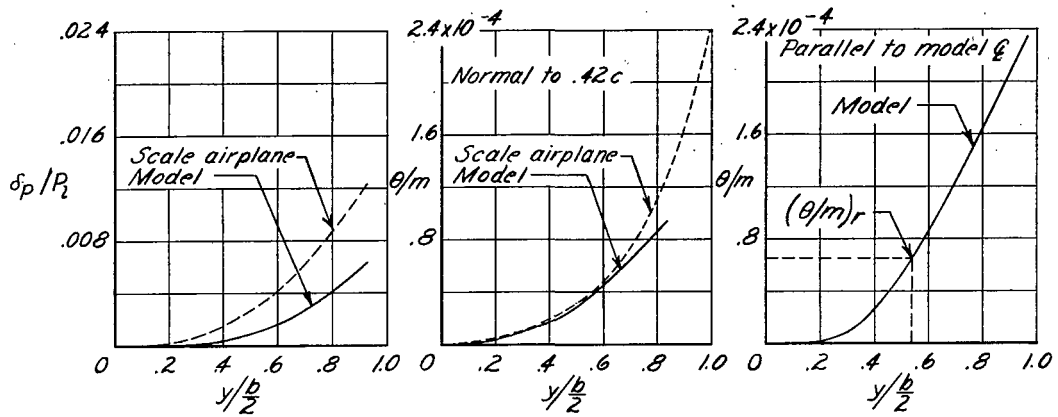
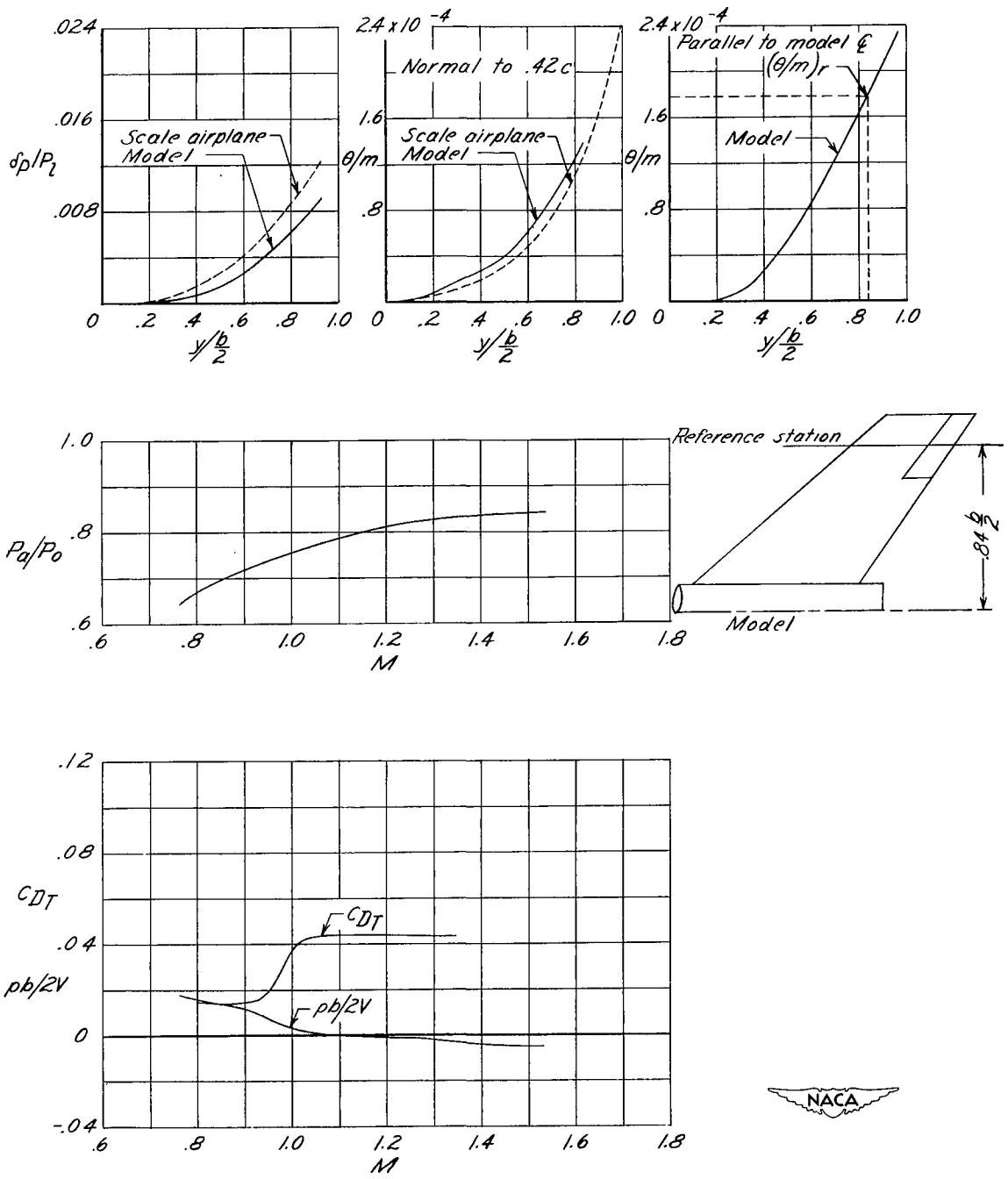


Figure 6.- Typical structural test setup.



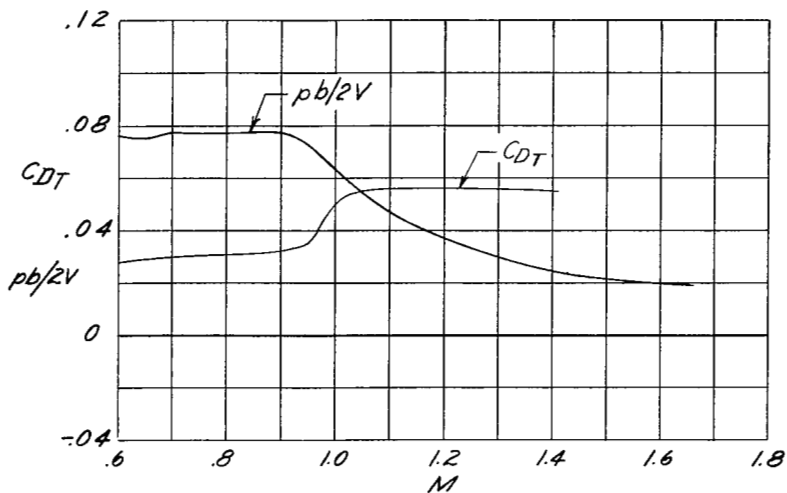
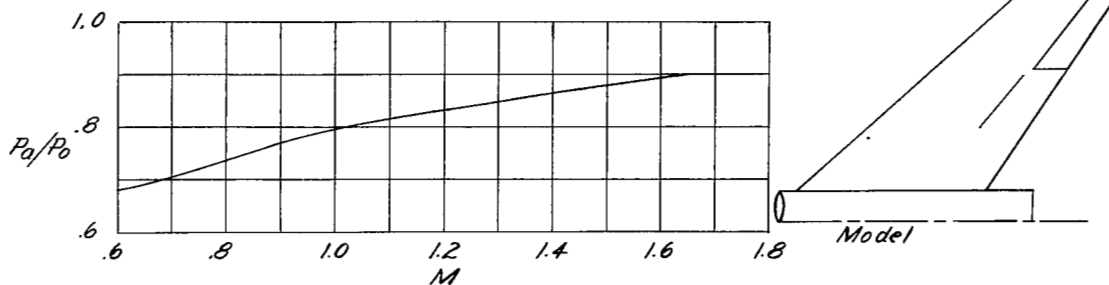
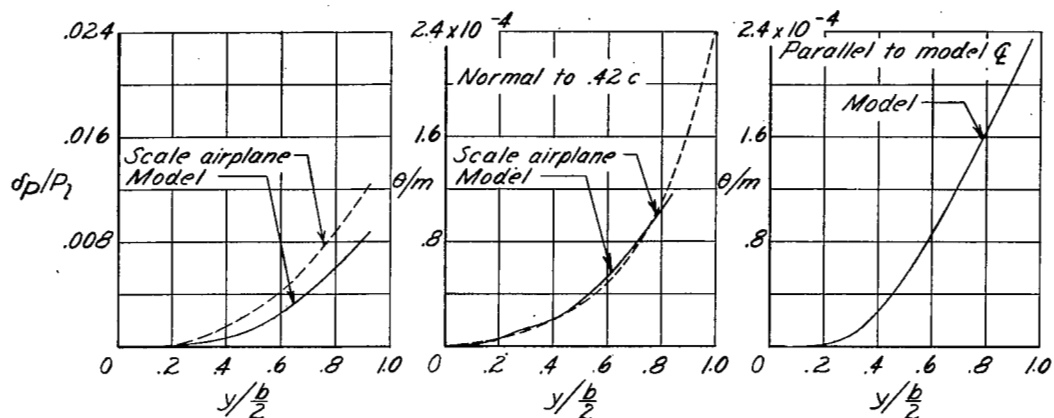
(a) Spoiler A on flexible wing; $(h/c)_{av} = 0.063$.

Figure 7.- Structural and aerodynamic data.



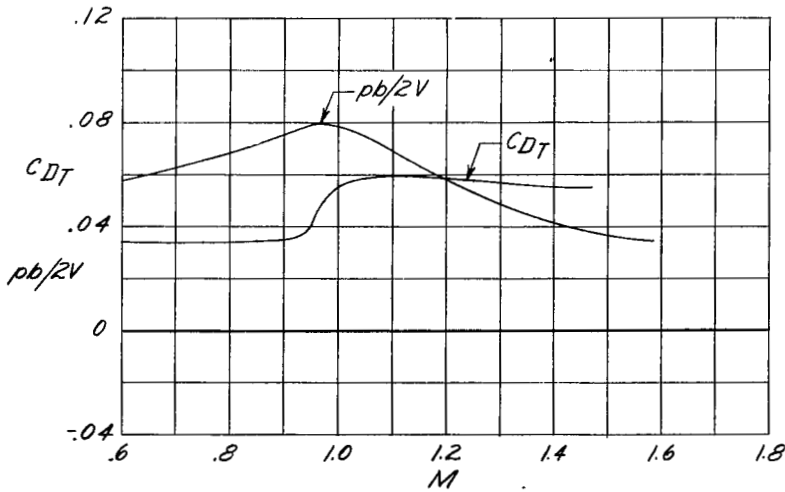
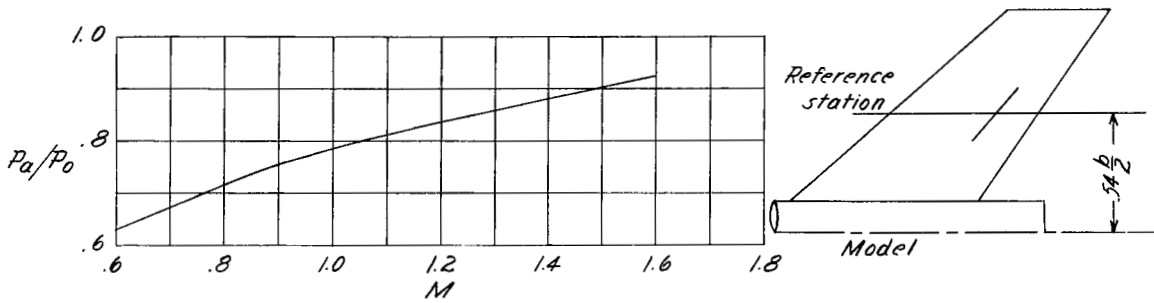
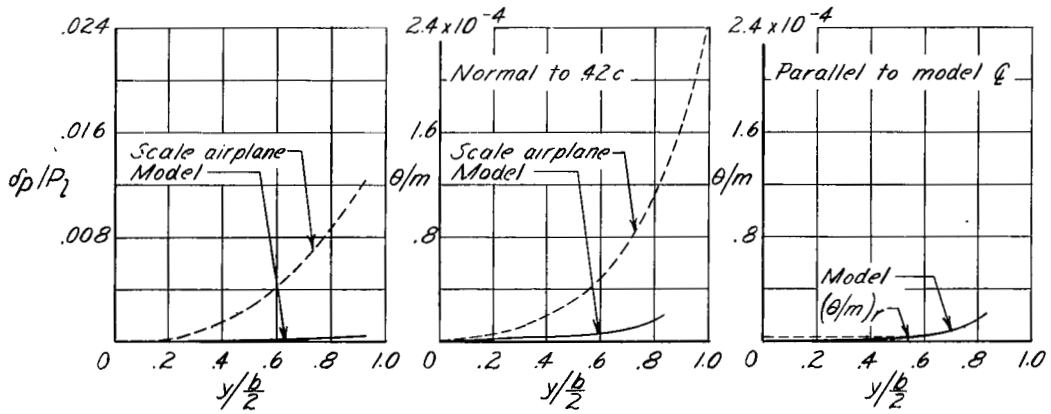
(b) Aileron on flexible wing; $\delta_a = 5.0^\circ$.

Figure 7.- Continued.



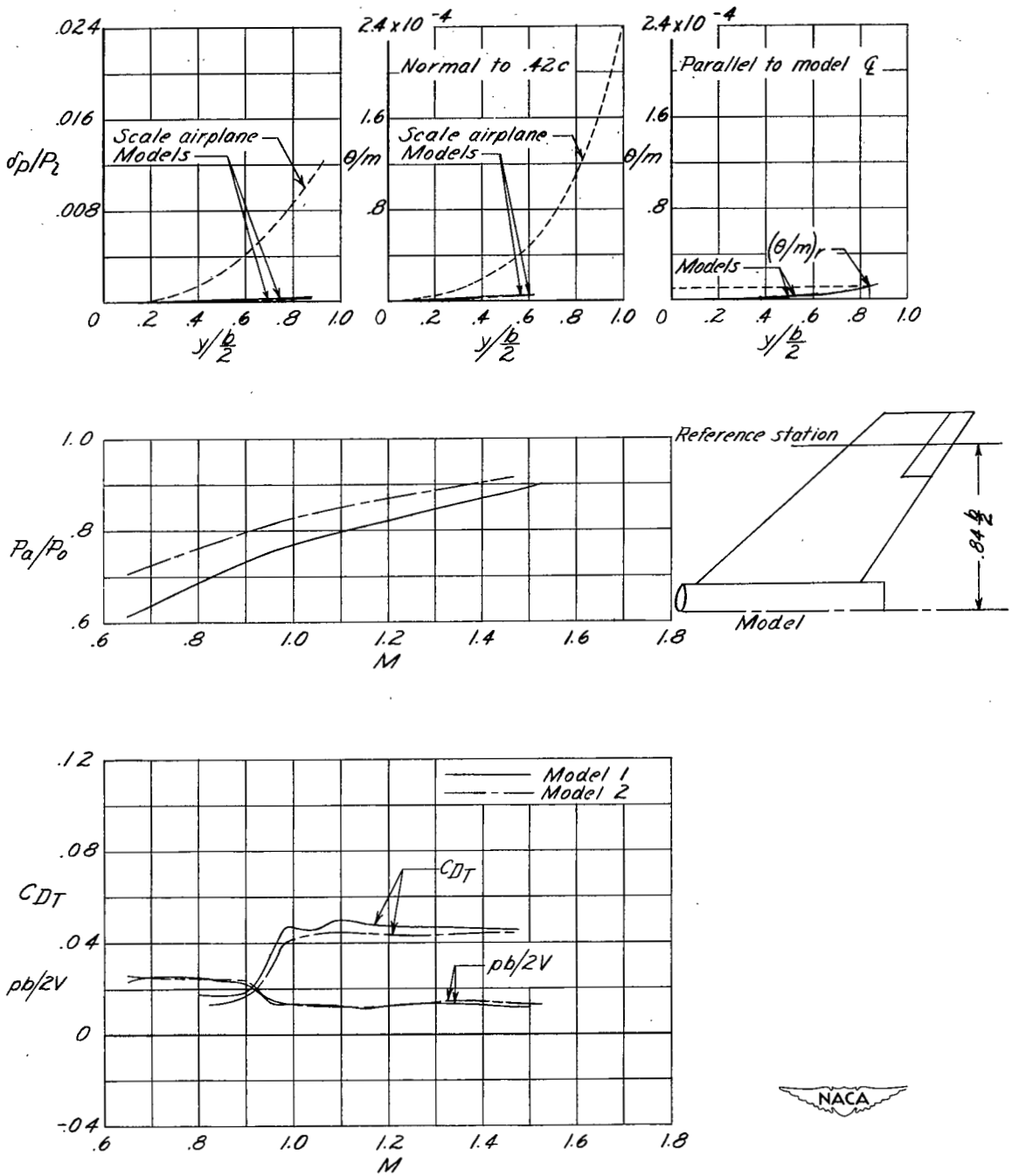
(c) Aileron and spoiler A on flexible wing; $\delta_a = 5.0^\circ$; $(h/c)_{av} = 0.063$.

Figure 7.- Continued.



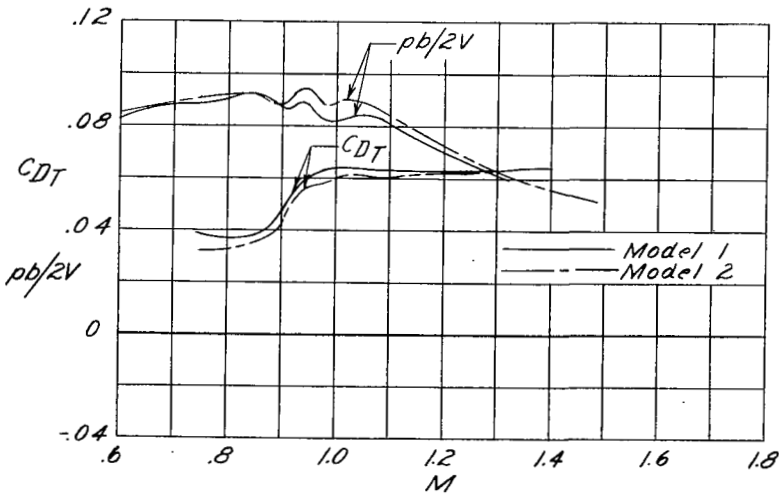
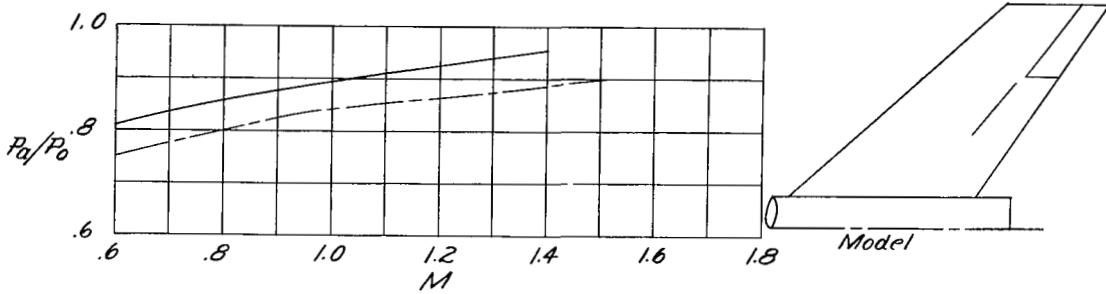
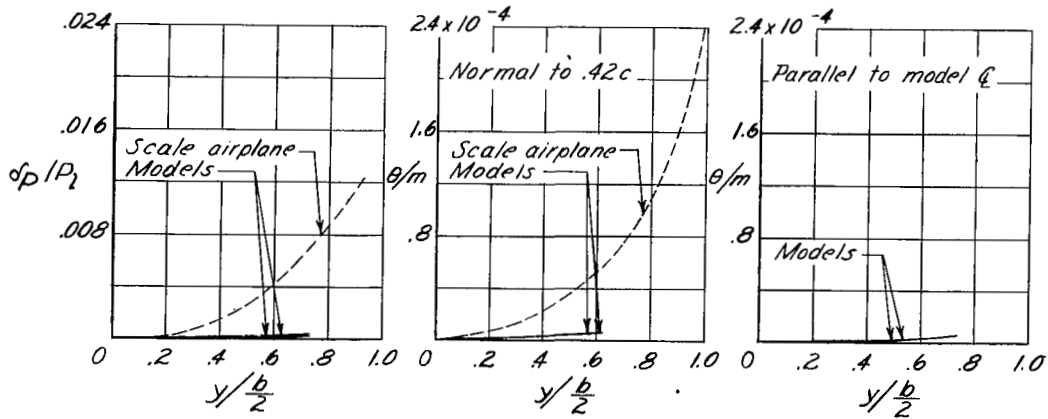
(d) Spoiler A on stiff wing; $(h/c)_{av} = 0.063$.

Figure 7.- Continued.



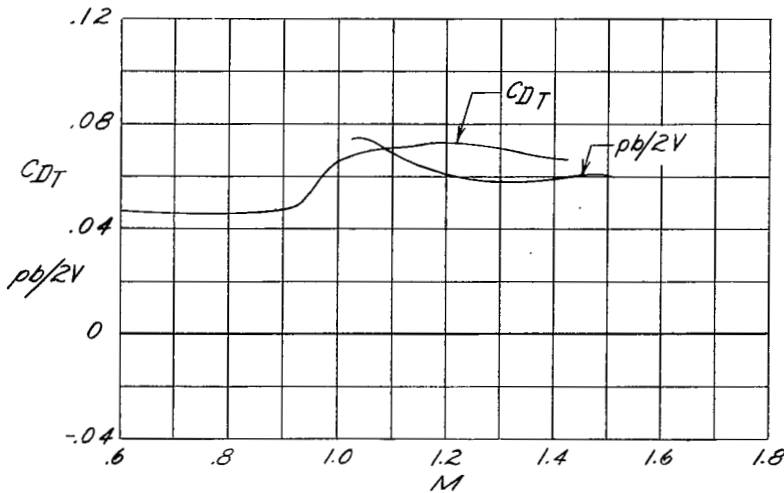
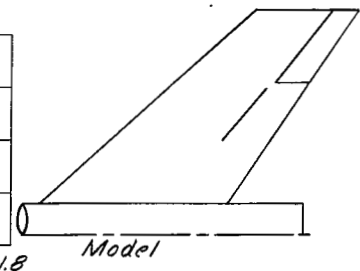
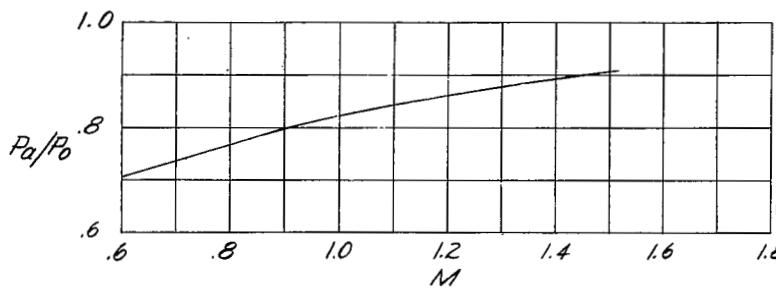
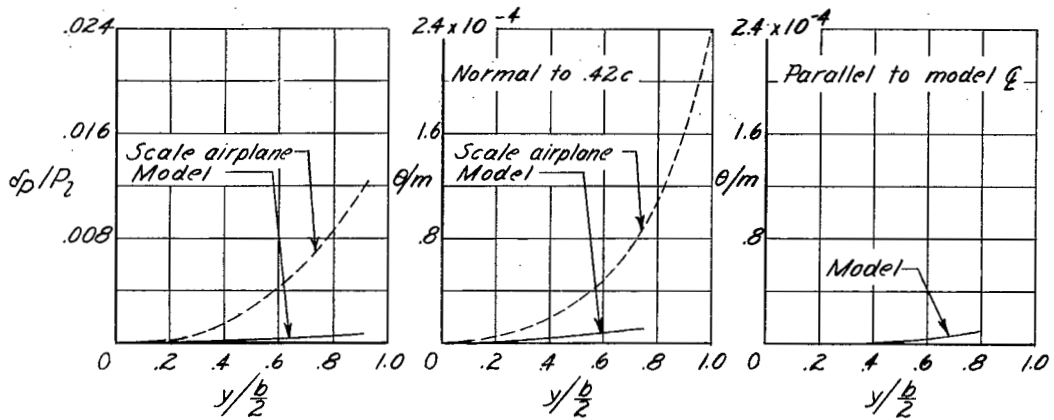
(e) Aileron on stiff wing; $\delta_a = 5.0^\circ$. Results shown for models 1 and 2.

Figure 7.- Continued.



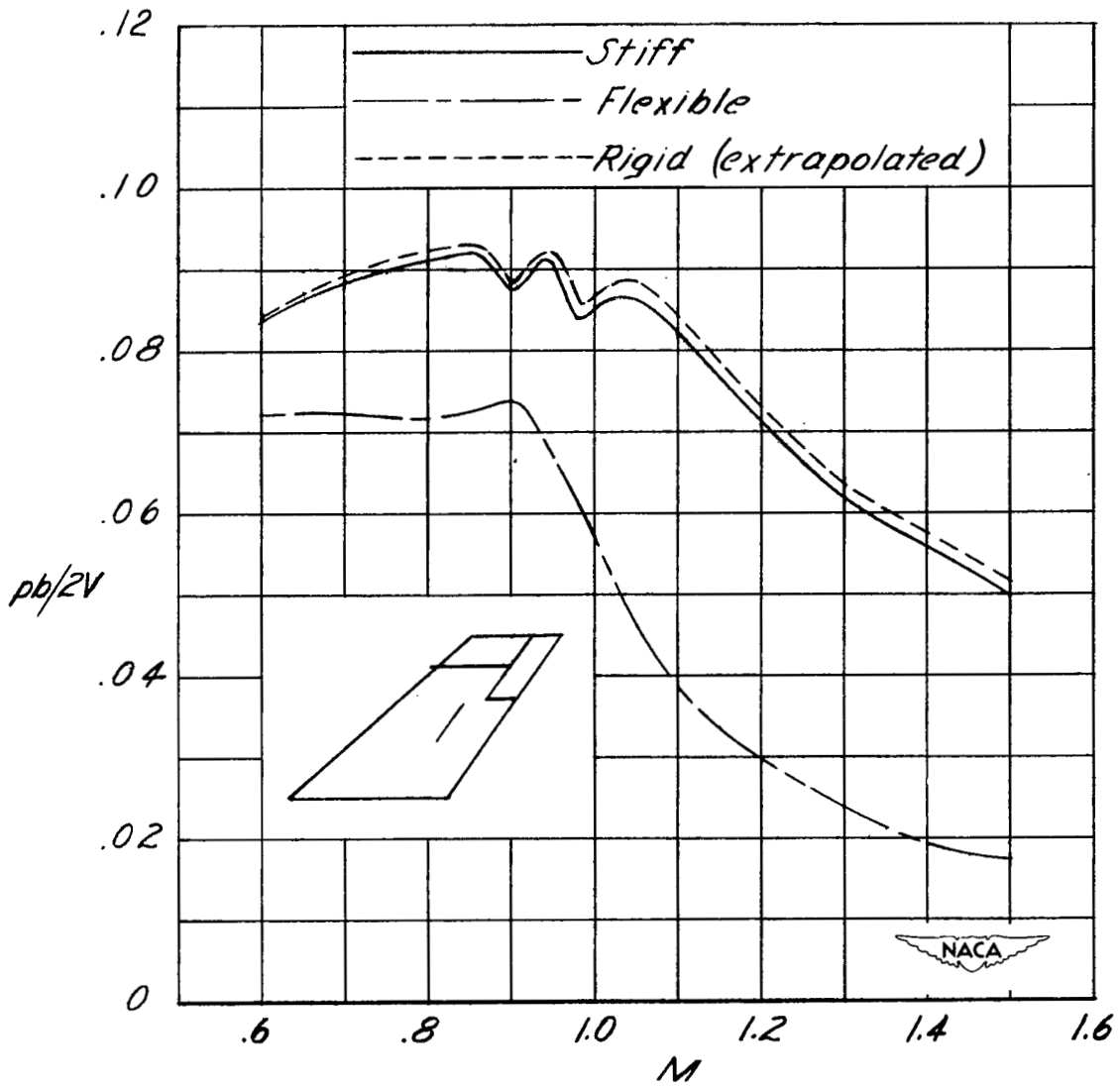
(f) Aileron and spoiler A on stiff wing; $\delta_a = 5.0^\circ$; $(h/c)_{av} = 0.063$. Results shown for models 1 and 2.

Figure 7.- Continued.



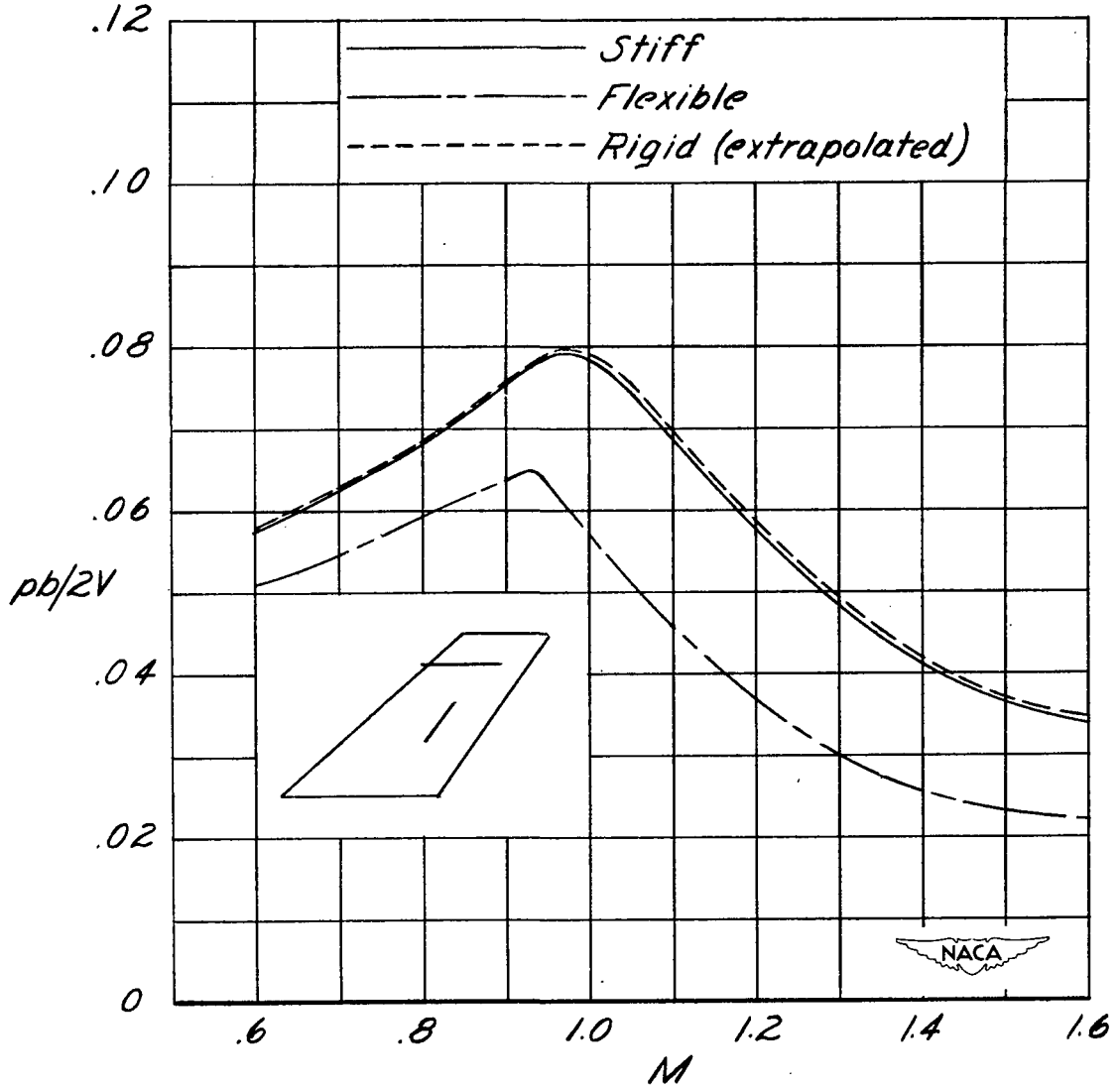
(g) Aileron and spoiler B on stiff wing; $\delta_a = 5.0^\circ$; $(h/c)_{av} = 0.061$.

Figure 7.- Concluded.



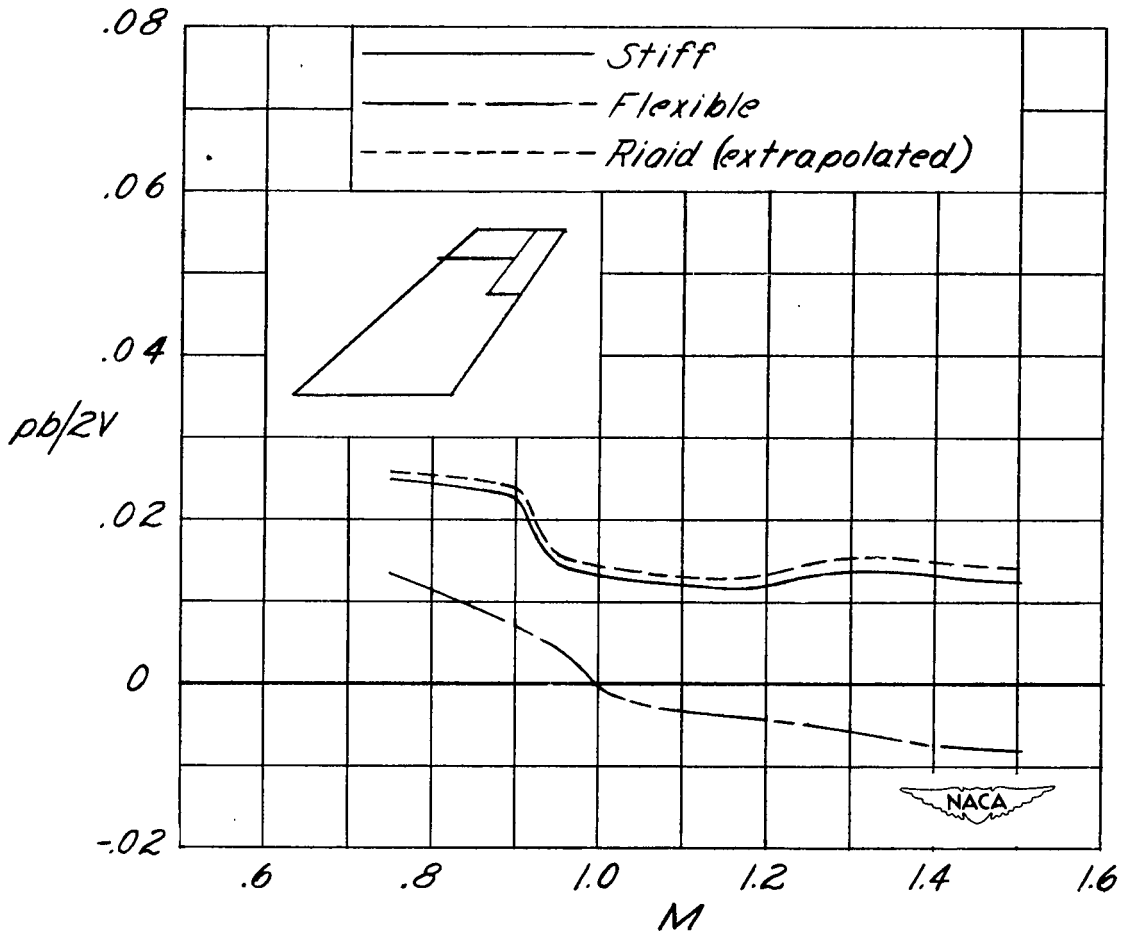
(a) Aileron and spoiler A; $\delta_a = 5.0^\circ$; $(h/c)_{AV} = 0.063$.

Figure 8.- Effect of wing flexibility upon variation of rolling effectiveness with Mach number. Sea-level conditions.



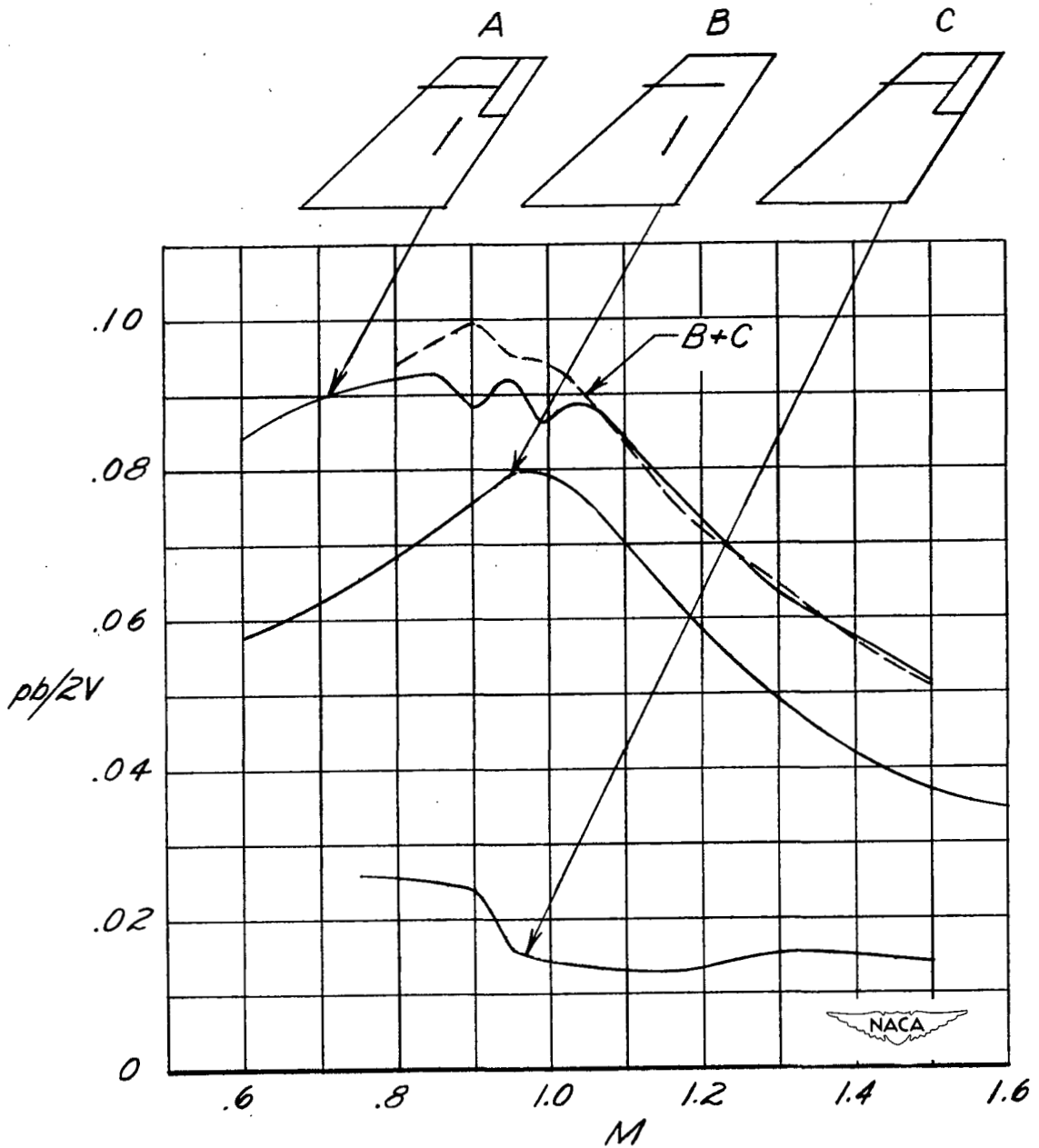
(b) Spoiler A; $(h/c)_{av} = 0.063$.

Figure 8.- Continued.



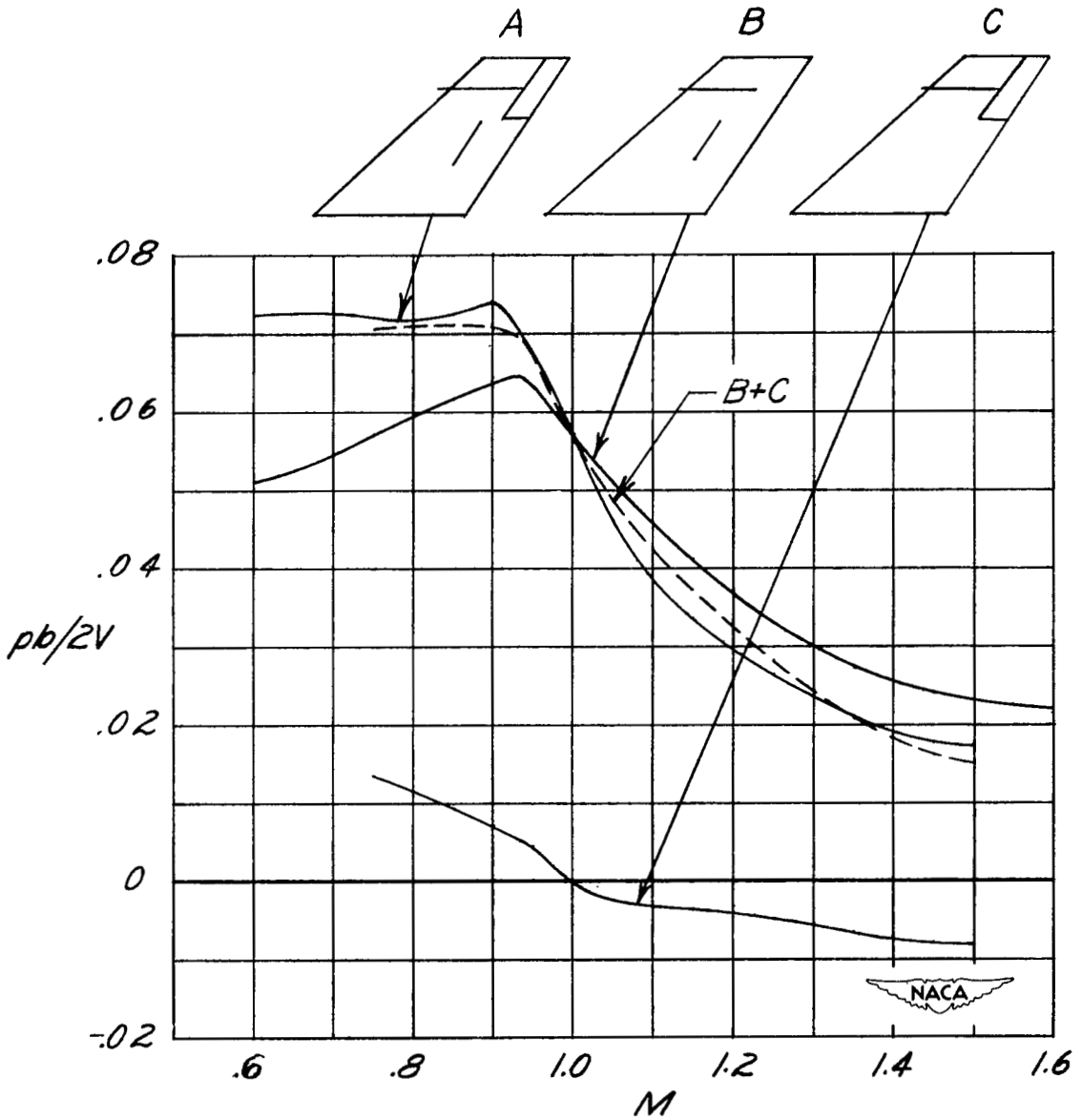
(c) Aileron; $\delta_a = 5.0^\circ$.

Figure 8.- Concluded.



(a) Extrapolated rigid-wing values.

Figure 9.- Effect of control configuration upon variation of rolling effectiveness with Mach number. Aileron and/or spoiler A. $\delta_a = 5.0^\circ$; $(h/c)_{av} = 0.063$ where deflected.



(b) Flexible-wing models at sea-level conditions.

Figure 9.- Concluded.

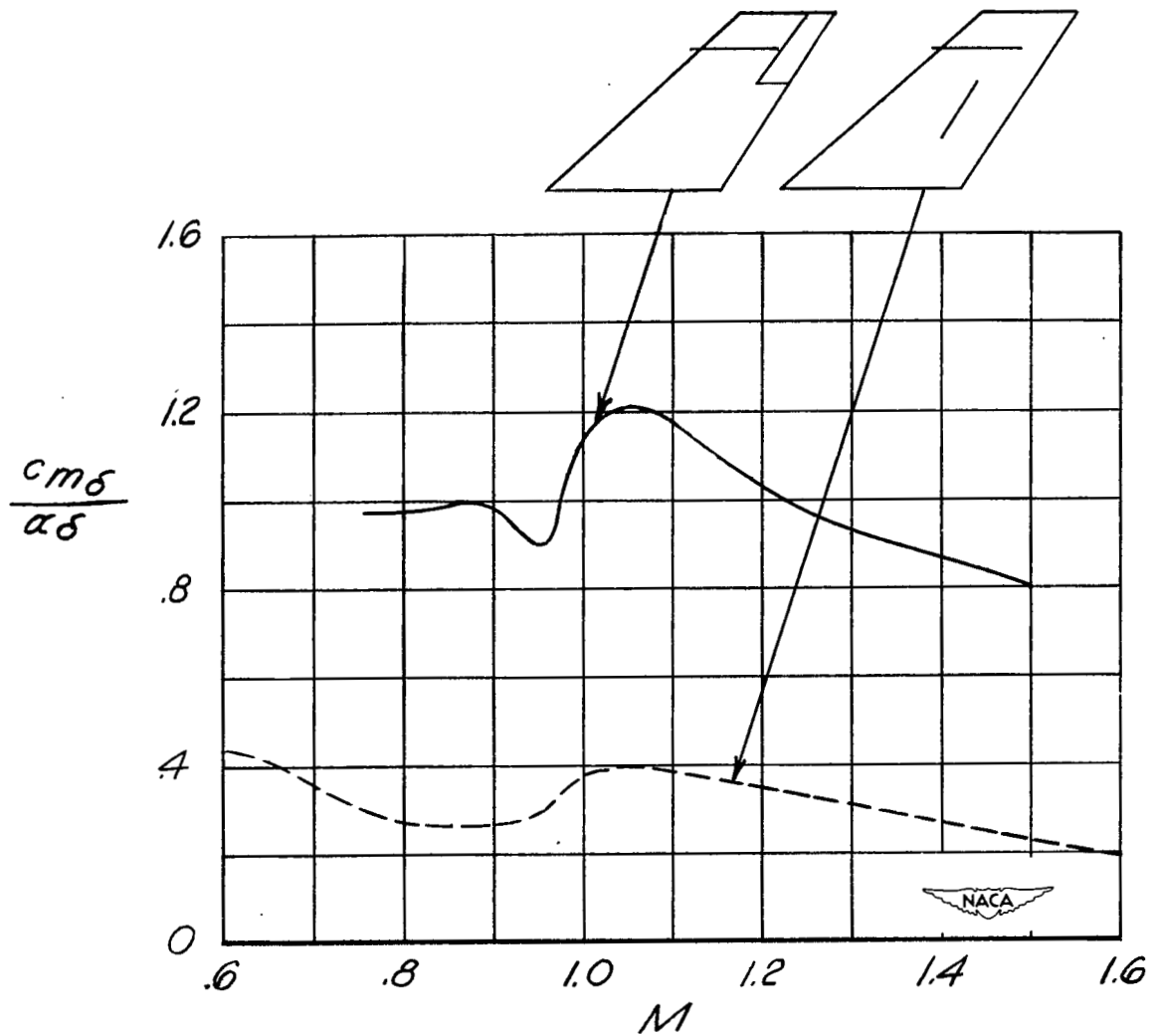
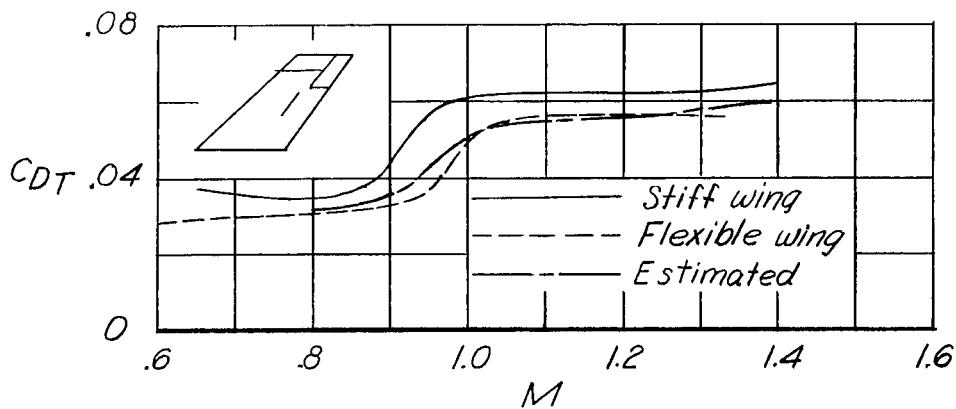
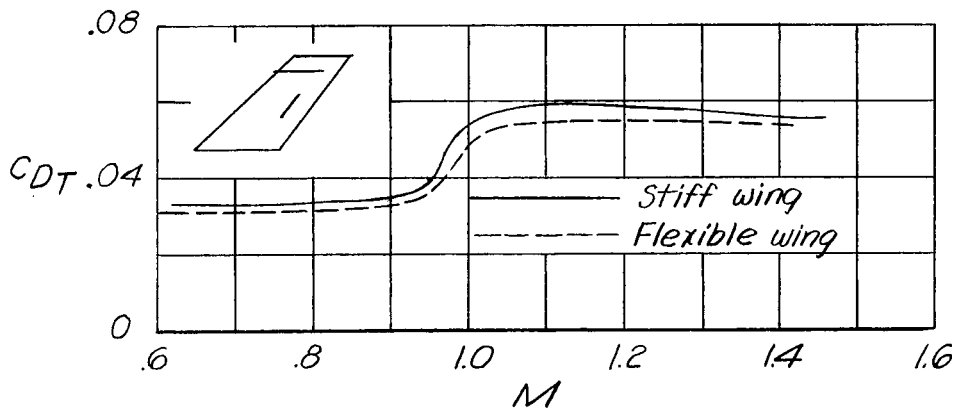


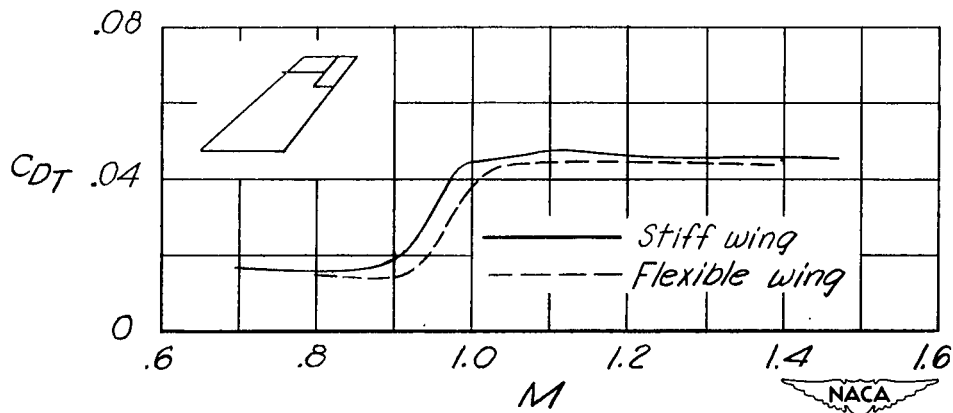
Figure 10.- Variation of effective twisting-moment coefficient with Mach number for aileron and spoiler A.



(a) Aileron and spoiler A.

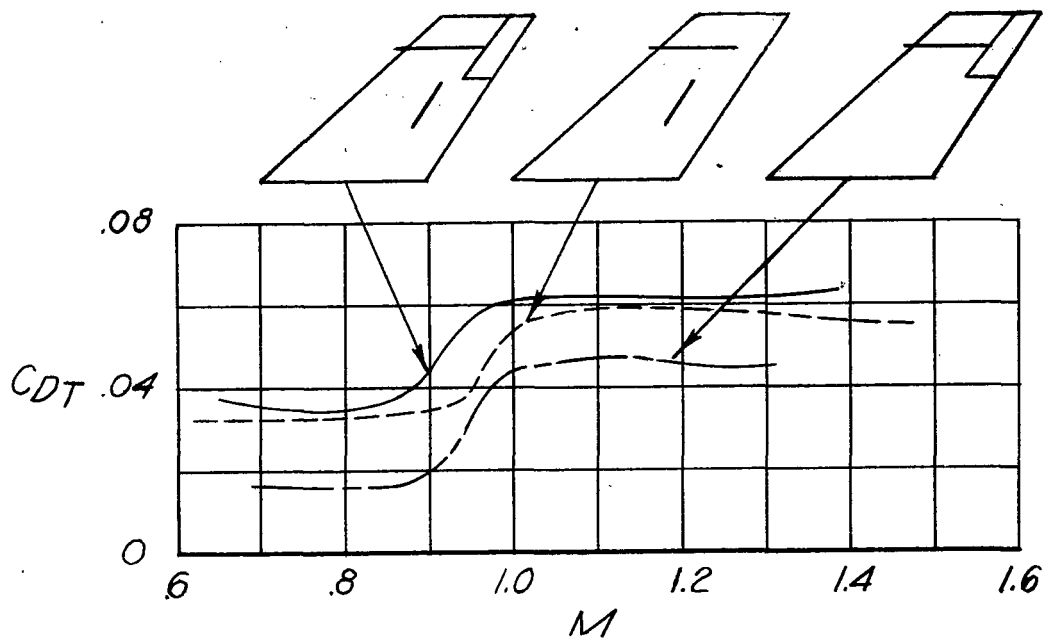


(b) Spoiler A.

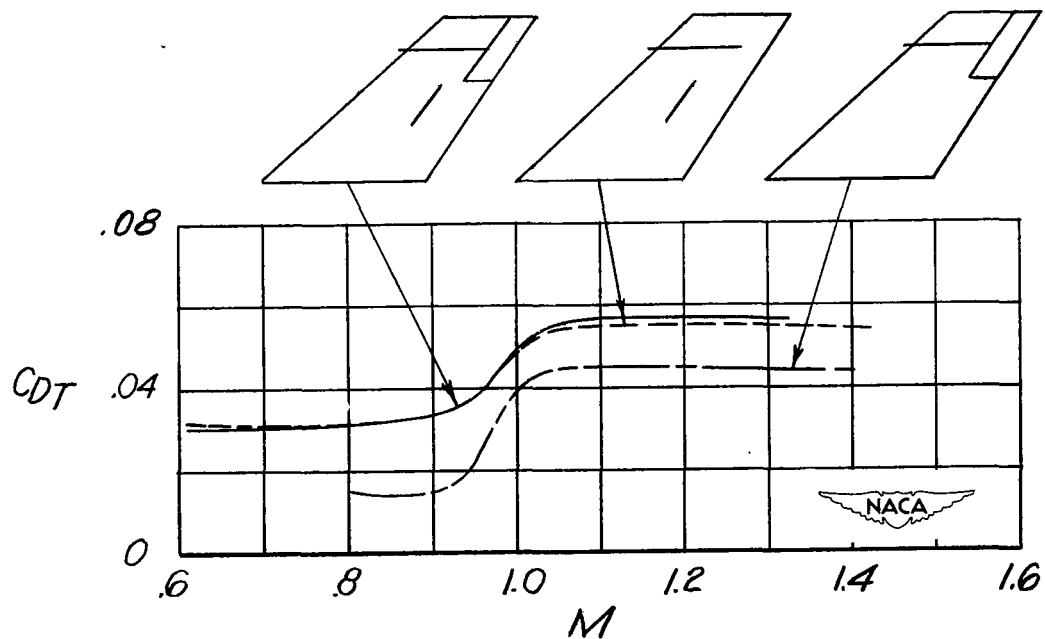


(c) Aileron.

Figure 11.- Effect of wing flexibility upon variation of total drag coefficient with Mach number.



(a) Stiff-wing models.



(b) Flexible-wing models.

Figure 12.- Effect of control configuration upon variation of total drag coefficient with Mach number. Aileron and/or spoiler A.

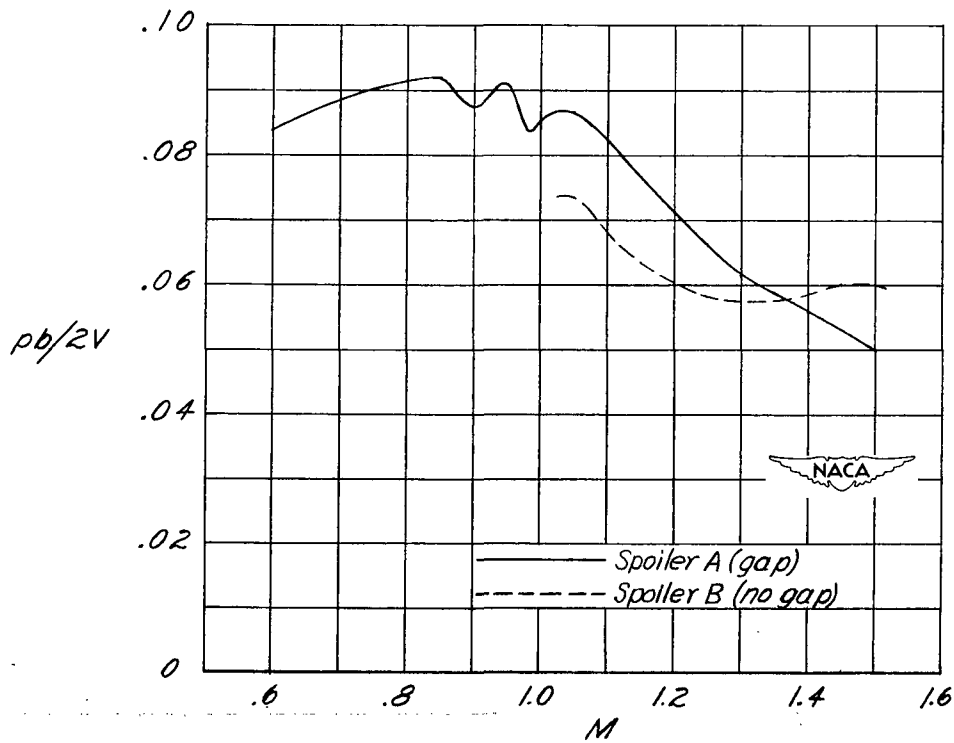
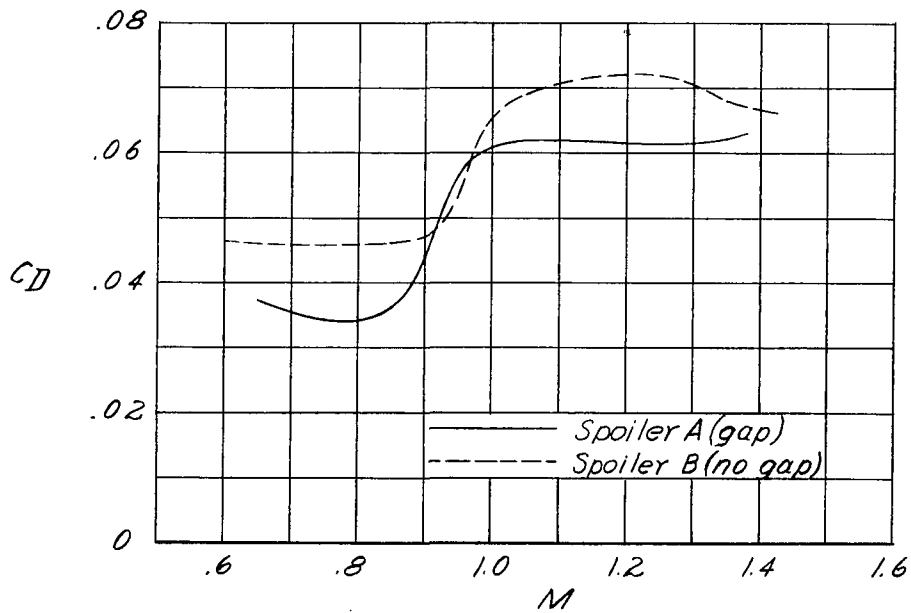


Figure 13.- Comparison of the variation of rolling effectiveness and total drag coefficient with Mach number for two types of spoilers on stiff-wing models. Basic data uncorrected for altitude.

SECURITY INFORMATION

NASA Technical Library



3 1176 01437 7502

